

# Improved Measurement of the Branching Fraction and Energy Spectrum of $\eta'$ from $\Upsilon(1S)$ Decays\*

O. Aquines,<sup>1</sup> Z. Li,<sup>1</sup> A. Lopez,<sup>1</sup> S. Mehrabyan,<sup>1</sup> H. Mendez,<sup>1</sup> J. Ramirez,<sup>1</sup>  
 G. S. Huang,<sup>2</sup> D. H. Miller,<sup>2</sup> V. Pavlunin,<sup>2</sup> B. Sanghi,<sup>2</sup> I. P. J. Shipsey,<sup>2</sup> B. Xin,<sup>2</sup>  
 G. S. Adams,<sup>3</sup> M. Anderson,<sup>3</sup> J. P. Cummings,<sup>3</sup> I. Danko,<sup>3</sup> J. Napolitano,<sup>3</sup>  
 Q. He,<sup>4</sup> J. Insler,<sup>4</sup> H. Muramatsu,<sup>4</sup> C. S. Park,<sup>4</sup> E. H. Thorndike,<sup>4</sup> F. Yang,<sup>4</sup>  
 T. E. Coan,<sup>5</sup> Y. S. Gao,<sup>5</sup> F. Liu,<sup>5</sup> M. Artuso,<sup>6</sup> S. Blusk,<sup>6</sup> J. Butt,<sup>6</sup> J. Li,<sup>6</sup> N. Menaa,<sup>6</sup>  
 R. Mountain,<sup>6</sup> S. Nisar,<sup>6</sup> K. Randrianarivony,<sup>6</sup> R. Redjimi,<sup>6</sup> R. Sia,<sup>6</sup> T. Skwarnicki,<sup>6</sup>  
 S. Stone,<sup>6</sup> J. C. Wang,<sup>6</sup> K. Zhang,<sup>6</sup> S. E. Csorna,<sup>7</sup> G. Bonvicini,<sup>8</sup> D. Cinabro,<sup>8</sup>  
 M. Dubrovin,<sup>8</sup> A. Lincoln,<sup>8</sup> D. M. Asner,<sup>9</sup> K. W. Edwards,<sup>9</sup> R. A. Briere,<sup>10</sup>  
 I. Brock,<sup>10</sup> J. Chen,<sup>10</sup> T. Ferguson,<sup>10</sup> G. Tatishvili,<sup>10</sup> H. Vogel,<sup>10</sup> M. E. Watkins,<sup>10</sup>  
 J. L. Rosner,<sup>11</sup> N. E. Adam,<sup>12</sup> J. P. Alexander,<sup>12</sup> K. Berkelman,<sup>12</sup> D. G. Cassel,<sup>12</sup>  
 J. E. Duboscq,<sup>12</sup> K. M. Ecklund,<sup>12</sup> R. Ehrlich,<sup>12</sup> L. Fields,<sup>12</sup> R. S. Galik,<sup>12</sup>  
 L. Gibbons,<sup>12</sup> R. Gray,<sup>12</sup> S. W. Gray,<sup>12</sup> D. L. Hartill,<sup>12</sup> B. K. Heltsley,<sup>12</sup>  
 D. Hertz,<sup>12</sup> C. D. Jones,<sup>12</sup> J. Kandaswamy,<sup>12</sup> D. L. Kreinick,<sup>12</sup> V. E. Kuznetsov,<sup>12</sup>  
 H. Mahlke-Krüger,<sup>12</sup> P. U. E. Onyisi,<sup>12</sup> J. R. Patterson,<sup>12</sup> D. Peterson,<sup>12</sup> J. Pivarski,<sup>12</sup>  
 D. Riley,<sup>12</sup> A. Ryd,<sup>12</sup> A. J. Sadoff,<sup>12</sup> H. Schwarthoff,<sup>12</sup> X. Shi,<sup>12</sup> S. Stroiney,<sup>12</sup>  
 W. M. Sun,<sup>12</sup> T. Wilksen,<sup>12</sup> M. Weinberger,<sup>12</sup> S. B. Athar,<sup>13</sup> R. Patel,<sup>13</sup> V. Potlia,<sup>13</sup>  
 J. Yelton,<sup>13</sup> P. Rubin,<sup>14</sup> C. Cawfield,<sup>15</sup> B. I. Eisenstein,<sup>15</sup> I. Karliner,<sup>15</sup> D. Kim,<sup>15</sup>  
 N. Lowrey,<sup>15</sup> P. Naik,<sup>15</sup> C. Sedlack,<sup>15</sup> M. Selen,<sup>15</sup> E. J. White,<sup>15</sup> J. Wiss,<sup>15</sup>  
 M. R. Shepherd,<sup>16</sup> D. Besson,<sup>17</sup> T. K. Pedlar,<sup>18</sup> D. Cronin-Hennessy,<sup>19</sup> K. Y. Gao,<sup>19</sup>  
 D. T. Gong,<sup>19</sup> J. Hietala,<sup>19</sup> Y. Kubota,<sup>19</sup> T. Klein,<sup>19</sup> B. W. Lang,<sup>19</sup> R. Poling,<sup>19</sup>  
 A. W. Scott,<sup>19</sup> A. Smith,<sup>19</sup> P. Zweber,<sup>19</sup> S. Dobbs,<sup>20</sup> Z. Metreveli,<sup>20</sup> K. K. Seth,<sup>20</sup>  
 A. Tomaradze,<sup>20</sup> J. Ernst,<sup>21</sup> H. Severini,<sup>22</sup> S. A. Dytman,<sup>23</sup> W. Love,<sup>23</sup> and V. Savinov<sup>23</sup>

(CLEO Collaboration)

<sup>1</sup>University of Puerto Rico, Mayaguez, Puerto Rico 00681

<sup>2</sup>Purdue University, West Lafayette, Indiana 47907

<sup>3</sup>Rensselaer Polytechnic Institute, Troy, New York 12180

<sup>4</sup>University of Rochester, Rochester, New York 14627

<sup>5</sup>Southern Methodist University, Dallas, Texas 75275

<sup>6</sup>Syracuse University, Syracuse, New York 13244

<sup>7</sup>Vanderbilt University, Nashville, Tennessee 37235

<sup>8</sup>Wayne State University, Detroit, Michigan 48202

<sup>9</sup>Carleton University, Ottawa, Ontario, Canada K1S 5B6

<sup>10</sup>Carnegie Mellon University, Pittsburgh, Pennsylvania 15213

<sup>11</sup>Enrico Fermi Institute, University of Chicago, Chicago, Illinois 60637

<sup>12</sup>Cornell University, Ithaca, New York 14853

<sup>13</sup>University of Florida, Gainesville, Florida 32611

<sup>14</sup>George Mason University, Fairfax, Virginia 22030

<sup>15</sup>University of Illinois, Urbana-Champaign, Illinois 61801

<sup>16</sup>Indiana University, Bloomington, Indiana 47405

<sup>17</sup>University of Kansas, Lawrence, Kansas 66045

<sup>18</sup>Luther College, Decorah, Iowa 52101

<sup>19</sup>University of Minnesota, Minneapolis, Minnesota 55455

<sup>20</sup>*Northwestern University, Evanston, Illinois 60208*

<sup>21</sup>*State University of New York at Albany, Albany, New York 12222*

<sup>22</sup>*University of Oklahoma, Norman, Oklahoma 73019*

<sup>23</sup>*University of Pittsburgh, Pittsburgh, Pennsylvania 15260*

(Dated: July 25, 2006)

## Abstract

We present an improved measurement of the  $\eta'$  meson energy spectrum in  $\Upsilon(1S)$  decays, using  $1.2 \text{ fb}^{-1}$  of data taken at the  $\Upsilon(1S)$  center-of-mass energy with the CLEO III detector. We compare our results with models of  $\eta'$  gluonic form factor that have been suggested to explain the unexpectedly large  $B \rightarrow \eta' X_s$  rate. Models based on perturbative QCD fail to fit the data for large  $\eta'$  energies, showing that Standard Model strong interaction dynamics is not likely to provide an explanation for the large rate of high energy  $\eta'$  observed in  $B$  decays.

---

\*Submitted to the 33<sup>rd</sup> International Conference on High Energy Physics, July 26 - August 2, 2006, Moscow

## I. INTRODUCTION

A surprisingly large rate for  $B \rightarrow \eta' X_s$ , with high momentum  $\eta'$ , ( $p_{\eta'}=2 - 2.7$  GeV/c), was observed by CLEO [1, 2] and confirmed by BaBar [3]. This result motivated intense theoretical activity because new physics could account for such an enhancement. However, Standard Model explanations have also been proposed. For example, Atwood and Soni [4] argued that the observed excess is due to an enhanced  $b \rightarrow sg$  penguin diagram, complemented by a strong  $\eta'gg^*$  coupling, induced by the gluonic content of the  $\eta'$  wave function. Fig. 1 (left) shows the corresponding Feynman diagram. The high  $q^2$  region of the  $g^*g\eta'$  vertex function involved in this process also affects fast  $\eta'$  production in  $\Upsilon(1S)$  decay [5, 6], whose relevant diagram is shown in Figure 1 (right). Thus a precise measurement of the  $\eta'$  inclusive spectra from the process  $\Upsilon(1S) \rightarrow ggg^* \rightarrow \eta'X$  provides valuable information towards our understanding of important  $B$  meson decays.

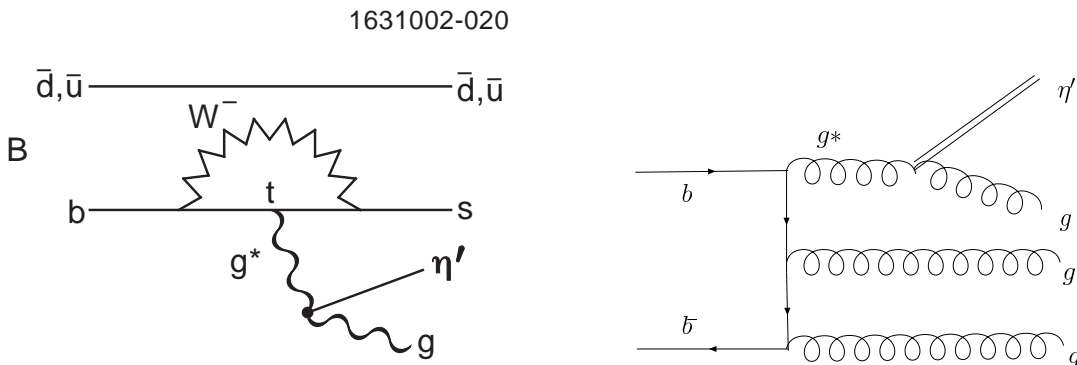


FIG. 1: Feynman Diagram for  $b \rightarrow sg$  (left) and  $\Upsilon(1S) \rightarrow ggg^* \rightarrow \eta'X$  (right).

The effective vertex function  $\eta'gg^*$  can be written as [4]:

$$H(q^2)\delta^{ab}\varepsilon_{\alpha\beta\mu\nu}q^\alpha k^\beta\varepsilon_1^\mu\varepsilon_2^\nu, \quad (1)$$

where  $q$  is the ( $g^*$ ) virtual gluon's four-momentum,  $k$  is the ( $g$ ) “on-shell” gluon's momentum ( $k^2 = 0$ ),  $a, b$  represent color indices,  $\varepsilon_1^\mu, \varepsilon_2^\nu$  are the polarization vectors of the two gluons, and  $H(q^2)$  is the  $g^*g\eta'$  transition form factor. Different assumptions on its  $q^2$  dependence have been proposed [4, 6, 7, 8, 9, 10].

While ARGUS was the first experiment to study the inclusive  $\eta'$  production at the  $\Upsilon(1S)$  [11], CLEO II [12] was the first experiment to have sufficient statistics to measure inclusive  $\eta'$  production from the subprocess  $\Upsilon(1S) \rightarrow ggg$ . These data ruled out a class of form factors characterized by a very weak  $q^2$  dependence [4, 7]. Intense theoretical activity has followed [6, 9, 10] to derive the perturbative QCD form factors from models of the  $\eta'$  wave function. Attempts to use CLEO II data to constrain the model parameters [13] were not conclusive, due to the limited statistics at the end point of the  $\eta'$  spectrum. Moreover, the order of the perturbative expansion necessary to achieve a good representation of the data was not clearly defined [13]. Thus an improved measurement, based on a higher statistics sample, is important to settle these issues. This work reports a new measurement of the inclusive  $\eta'$  spectrum from the process  $\Upsilon(1S) \rightarrow ggg^* \rightarrow \eta'X$  based on the largest  $\Upsilon(1S)$  sample presently available, more than a factor of 11 higher than the previous study [12]. Thus the measured high energy distribution function provides a much more stringent constraint.

## II. DATA SAMPLE AND ANALYSIS METHOD

We use  $1.2 \text{ fb}^{-1}$  of CLEO III data recorded at the  $\Upsilon(1S)$  resonance, at 9.46 GeV center-of-mass energy, containing  $21.2 \times 10^6$  events and off-resonance continuum data collected at center-of-mass energies of 10.54 GeV ( $2.3 \text{ fb}^{-1}$ ).

The CLEO III detector includes a high resolution tracking system [14], a state of the art CsI electromagnetic calorimeter [15], and a Ring Imaging Cherenkov (RICH) hadron identification system [16]. The CsI calorimeter measures the photon energies with a resolution of 2.2% at  $E = 1 \text{ GeV}$  and 5% at  $E=100 \text{ MeV}$ . The tracking system provides also charged particle discrimination, through the measurement of the specific ionization  $dE/dx$ .

We detect  $\eta'$  mesons through the channel  $\eta' \rightarrow \eta\pi^+\pi^-$  and  $\eta \rightarrow \gamma\gamma$ . The branching fractions for these processes are  $(44.5 \pm 1.4)\%$  and  $(39.38 \pm 0.26)\%$  respectively. We identify single photons based on their shower shape. The photon four-vectors are constrained to have invariant mass equal to the nominal  $\eta$  mass. Subsequently,  $\eta$  candidates are combined with two oppositely charged tracks to form an  $\eta'$ . Loose  $\pi$  consistency criteria based on  $dE/dx$  measurements are applied to the charged tracks.

The gluonic  $\eta'$  production at the  $\Upsilon(1S)$  is expected to be dominant only at very high  $q^2$ , or, equivalently, at high  $\eta'$  scaled energy  $Z$ , where  $Z$  is defined as

$$Z \equiv \frac{E_{\eta'}}{E_{\text{beam}}} = \frac{E_{\eta'}}{2M_{\Upsilon(1S)}}, \quad (2)$$

where  $E_{\eta'}$  is the  $\eta'$  energy and  $E_{\text{beam}}$  is the beam energy. Enhanced  $\eta'$  production at high  $Z$  would indicate a large  $\eta'g^*g$  coupling.

For low energy  $\eta'$ s, photons coming from low energy  $\pi^0$ s are a severe source of background. Thus a  $\pi^0$  veto is applied for  $Z < 0.5$ , whereby photon pairs that have an invariant mass consistent (within  $2.5 \sigma$ ) of the nominal  $\pi^0$  mass are not included as the candidate photons for  $\eta$  reconstruction. We consider only  $\eta'$  with scaled energy  $Z$  between 0.2 and 1 and divide this range into eight equal bins. Fig. 2 demonstrates the extraction of the  $\eta'$  yields in these bins for the  $\Upsilon(1S)$  sample. Fig. 3 shows the corresponding plots from the continuum sample taken at a center-of-mass energy of 10.54 GeV. In order to derive the  $\eta'$  signal yields, we fit the mass difference spectra  $\Delta M_{\eta'\eta} \equiv M(\pi^+\pi^-\eta) - M(\eta)$  in each  $Z$  bin with a Gaussian function representing the signal, and a polynomial background. The Gaussian is used only to define a  $\pm 2.5\sigma$  signal interval. Then the  $\eta'$  yield in this interval is evaluated counting events in the signal window, after subtracting the background estimate obtained from the fit function. As the signal is not described well by a single Gaussian function, this procedure minimizes systematic uncertainties associated with the choice of an alternative signal shape.

Information on the gluon coupling of the  $\eta'$  can be drawn only from the decay chain  $\Upsilon(1S) \rightarrow g^*gg \rightarrow \eta'X$ . Thus we need to subtract both continuum  $\eta'$  production and  $\eta'$  from the process  $\Upsilon(1S) \rightarrow \gamma^* \rightarrow q\bar{q}$ . The latter component is estimated using

$$\mathcal{B}(\Upsilon(1S) \rightarrow q\bar{q}) = R \cdot \mathcal{B}(\Upsilon(1S) \rightarrow \mu^+\mu^-) = (8.83 \pm 0.25)\%, \quad (3)$$

where  $R$  is the ratio between the hadronic cross section  $\gamma^* \rightarrow q\bar{q}$  and the di-muon cross section  $\gamma^* \rightarrow \mu^+\mu^-$  at an energy close to 9.46 GeV. We use  $R = 3.56 \pm 0.07$  [17] and  $\mathcal{B}(\Upsilon(1S) \rightarrow \mu^+\mu^-) = (2.48 \pm 0.05)\%$  [18].

The two dominant components of the  $\eta'$  spectrum have different topologies:  $\Upsilon(1S) \rightarrow ggg$  produces a spherical event topology, whereas  $q\bar{q}$  processes are more jet-like. This difference affects the corresponding reconstruction efficiencies. Fig. 4 shows the efficiencies obtained

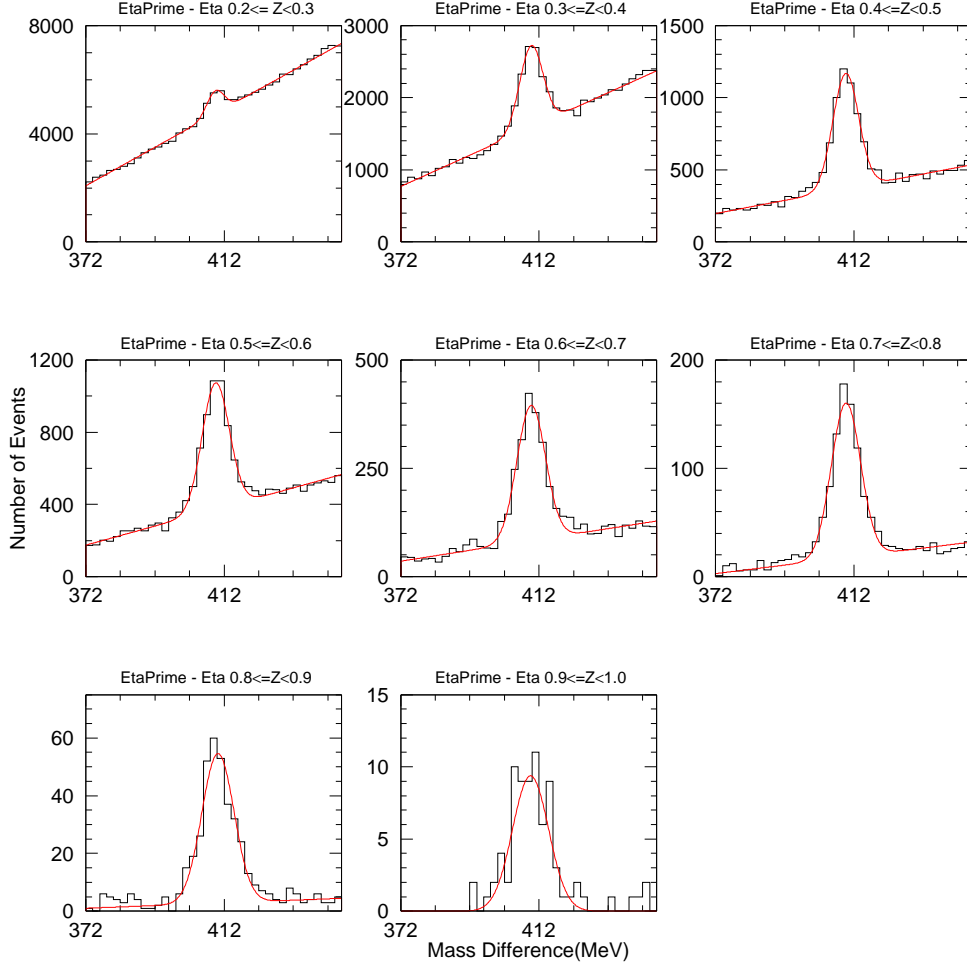


FIG. 2: The difference of the  $\eta\pi^+\pi^-$  and  $\eta$  invariant masses spectra in different  $Z$  ranges reconstructed from  $\Upsilon(1S)$  data, fit with a single Gaussian function for the signal and a first order polynomial for the background.

for the two event topologies with CLEO III Monte Carlo studies. We use GEANT-based [19] Monte Carlo samples, including  $\Upsilon(1S)$  and continuum samples. In order to use the continuum sample taken at 10.54 GeV center-of-mass energy for background subtraction, we develop a “mapping function”, to correct for the difference in phase space and  $Z$  range spanned in the two samples. The procedure is described in detail in Ref. [12]. By comparing the  $\eta'$  energy distribution functions for the Monte Carlo continuum samples at center-of-mass energies equal to 9.46 and 10.54 GeV, we obtain the mapping:

$$Z_{9.46} = -0.215 \times 10^{-2} + 1.2238 Z_{10.54} - 0.6879 (Z_{10.54})^2 + 0.8277 (Z_{10.54})^3 - 0.3606 (Z_{10.54})^4, \quad (4)$$

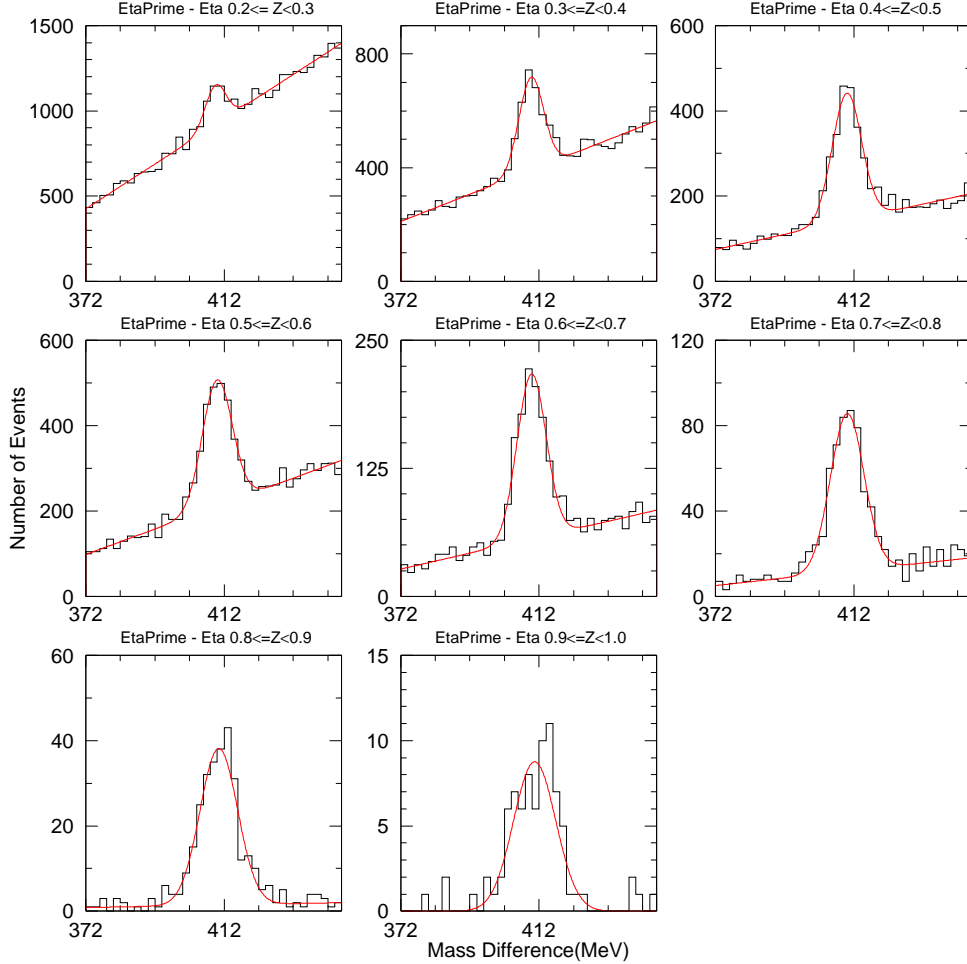


FIG. 3: The difference of the  $\eta\pi^+\pi^-$  and  $\eta$  invariant masses spectra in different  $Z$  ranges reconstructed from continuum data taken at a center-of-mass energy of 10.54 GeV, fit with a Single Gaussian function for the signal and a first order polynomial for the background.

where  $Z_{9,46}$  is the  $Z$  value used to subtract the continuum contribution, as mapped from  $Z_{10,54}$ , the measured  $Z$  in the continuum data taken at the center-of-mass energy equal to 10.54 GeV.

The  $\gamma gg/ggg$  cross section ratio is only about 3%, thus we make no attempt to subtract this term.

Upon correcting the raw yields with the corresponding efficiencies, the  $\eta'$  spectrum from the 3 gluon decay of the  $\Upsilon(1S)$  is extracted using the relationship:

$$N(\Upsilon(1S) \rightarrow ggg) = N_{\text{had}} - N(\gamma^* \rightarrow q\bar{q}) - N(\Upsilon(1S) \rightarrow q\bar{q}), \quad (5)$$

where  $N_{\text{had}}$  is the number of hadronic events in our sample, and  $N(\gamma^* \rightarrow q\bar{q})$  is the number of

continuum events estimated from the sample taken at 10.54 GeV, corrected for the luminosity difference between the resonance and continuum data, and the  $s$  dependence of the cross section for the process  $\gamma^* \rightarrow q\bar{q}$ . The component  $N(\Upsilon(1S)) \rightarrow q\bar{q}$  is estimated from  $N(\gamma^* \rightarrow q\bar{q})$  using the relationship:

$$\begin{aligned} N(\Upsilon(1S) \rightarrow q\bar{q}) &= N(\gamma^* \rightarrow q\bar{q}) \times R_{\text{ISR-OFF/ISR-ON}} \times \frac{\sigma_{\Upsilon(1S) \rightarrow q\bar{q}}}{\sigma_{e^+e^- \rightarrow q\bar{q}}} \\ &= N(\gamma^* \rightarrow q\bar{q}) \times R_{\text{ISR-OFF/ISR-ON}} \times \frac{\sigma_{\Upsilon(1S) \rightarrow \mu^+\mu^-}}{\sigma_{e^+e^- \rightarrow \mu^+\mu^-}}, \end{aligned} \quad (6)$$

where  $R_{\text{ISR-OFF/ISR-ON}}$  accounts for the difference between the  $\Upsilon(1S) \rightarrow q\bar{q} \rightarrow \eta'X$  and the  $\gamma^* \rightarrow q\bar{q} \rightarrow \eta'X$  spectra due to initial state radiation (ISR) effects, estimated using Monte Carlo continuum samples with and without ISR simulation, and  $\sigma(\Upsilon(1S) \rightarrow q\bar{q})/\sigma(e^+e^- \rightarrow q\bar{q})$  accounts for the relative cross section of these two processes. The correction factor  $R_{\text{ISR-OFF/ISR-ON}}$  differs from 1 by a few percent at low  $Z$  and as much as 25% at the end point of the  $\eta'$  energy. The cross sections used are  $\sigma(\Upsilon(1S) \rightarrow \mu^+\mu^-) = 0.502 \pm 0.010$  nb [18] and  $\sigma(e^+e^- \rightarrow \mu^+\mu^-)$  is 1.38 nb [20]. Fig. 5 shows the differential cross sections  $d\sigma/dZ$  for the processes  $\Upsilon(1S) \rightarrow ggg$ ,  $\Upsilon(1S) \rightarrow q\bar{q}$ , and  $\gamma^* \rightarrow q\bar{q}$ .

Theoretical predictions give the energy distribution function

$$\frac{dn}{dZ} \equiv \frac{1}{N(\Upsilon(1S) \rightarrow ggg)} \times \frac{dN(\Upsilon(1S) \rightarrow ggg)}{dZ};$$

we obtain the corresponding experimental quantity by dividing by the total number of  $N(\Upsilon(1S) \rightarrow ggg)$ , estimated by applying Eq. 5 without any  $Z$  restriction. Fig. 6.a) shows the  $\Upsilon(1S) \rightarrow ggg \rightarrow \eta'X$  energy distribution function, whereas Fig. 6.b) and c) show the corresponding distributions for  $\Upsilon(1S) \rightarrow q\bar{q} \rightarrow \eta'X$ , normalized with respect of the total number of  $\Upsilon(1S) \rightarrow q\bar{q}$  and  $\Upsilon(1S) \rightarrow \eta'X$ , normalized with respect to the total number of  $\Upsilon(1S)$ .

The inclusive  $\eta'$  production at the  $\Upsilon(1S)$  is expected to be dominated by the transition  $\Upsilon(1S) \rightarrow ggg^* \rightarrow \eta'X$  only at high  $\eta'$  energy. The energy at which this occurs cannot be predicted from first principle: an empirical criterion is the  $\chi^2$  of the theory fit to the data. For example, a numerical analysis of the CLEO II data [13] obtained a  $\chi^2$  of 2.4 for three degrees of freedom, using the 3 experimental points at  $Z \geq 0.7$ , and  $\approx 24$  for 4 degrees of freedom using the 4 points at  $Z \geq 0.6$ . Thus Ali and Parkhomenko concluded that the  $Z$  region likely to be dominated by the  $\Upsilon(1S) \rightarrow ggg^* \rightarrow \eta'X$  starts at  $Z \geq 0.7$ . Thus, we quote separately global branching fractions for  $\Upsilon(1S) \rightarrow \eta'X$  and the corresponding results for  $Z \geq 0.7$ .

Table I summarizes the dominant components of the systematic uncertainties. The systematic errors on the branching fractions from  $\eta'$  are  $\pm 8.1\%$  for  $q\bar{q}$ ,  $\pm 9.1\%$  for the  $ggg \rightarrow \eta'X$  for  $Z > 0.7$  and  $\pm 7.2\%$  for all other branching fractions.

Thus we obtain:

$$\begin{aligned} n(\Upsilon(1S) \rightarrow (ggg) \rightarrow \eta'X) &\equiv \frac{N(\Upsilon(1S) \rightarrow ggg \rightarrow \eta'X)}{N(\Upsilon(1S) \rightarrow ggg)} = (3.2 \pm 0.2 \pm 0.2)\%, \\ n(\Upsilon(1S) \rightarrow (q\bar{q}) \rightarrow \eta'X) &\equiv \frac{N(\Upsilon(1S) \rightarrow q\bar{q} \rightarrow \eta'X)}{N(\Upsilon(1S) \rightarrow q\bar{q})} = (3.8 \pm 0.2 \pm 0.3)\%, \\ n(\Upsilon(1S) \rightarrow \eta'X) &\equiv \frac{N(\Upsilon(1S) \rightarrow \eta'X)}{N(\Upsilon(1S))} = (3.0 \pm 0.2 \pm 0.2)\%. \end{aligned} \quad (7)$$

Sources	$ggg$ Sample ( $Z > 0.7$ )	$q\bar{q}$ Sample	All others
Reconstruction efficiency of $\pi^\pm$	2	2	2
Reconstruction efficiency of $\eta$	5	5	5
Number of $\eta'$ from fit	1	1	1
Total number of $\Upsilon(1S)$	1	1	1
$\mathcal{B}(\eta' \rightarrow \pi^+\pi^-\eta)$	3.4	3.4	3.4
$\mathcal{B}(\Upsilon(1S) \rightarrow q\bar{q})$	-	3	-
Ratio of integrated luminosity	1.9	1	-
$\sigma_{\Upsilon(1S) \rightarrow \mu^+\mu^-} \cdot \sigma_{e^+e^- \rightarrow \mu^+\mu^-}$	0.7	1.3	-
$\pi^0$ veto	-	1.7	0.4
Z mapping	6	3	3
Total	9.1	8.1	7.2

TABLE I: The components of the systematic errors (%) affecting the branching fractions reported in this paper.

The  $\Upsilon(1S) \rightarrow \eta' X$  branching fractions at high momentum ( $Z > 0.7$ ) are measured to be:

$$\begin{aligned}
n(\Upsilon(1S) \rightarrow (ggg) \rightarrow \eta' X)_{Z>0.7} &= 3.7 \pm 0.5 \pm 0.3) \times 10^{-4}, \\
n(\Upsilon(1S) \rightarrow (q\bar{q}) \rightarrow \eta' X)_{Z>0.7} &= (22.5 \pm 1.2 \pm 1.8) \times 10^{-4}, \\
n(\Upsilon(1S) \rightarrow \eta' X)_{Z>0.7} &= (5.1 \pm 0.4 \pm 0.4) \times 10^{-4}.
\end{aligned}
\tag{8}$$

### III. COMPARISON WITH THEORY AND CONCLUSIONS

A. Kagan [5] used the ratio  $R_{Z>0.7}$  defined as

$$R_{Z>0.7} \equiv \left[ \frac{n_{th}}{n_{exp}} \right]_{Z>0.7},
\tag{9}$$

to obtain a first rough discrimination between radically different  $q^2$  dependence between the form factors. At the time that Ref. [5] was published, the comparison was based on 90% c.l. upper limits on the data. This test repeated with our present data give values of  $R_{Z>0.7}$  equal to 74 for a representative slowly falling form factor [7], 25 for the intermediate form factor studied by Ref. [8], and 2 for the perturbative QCD inspired shape. Thus the last shape is the closest to the data, although not providing a perfect match.

Different approaches have been taken to implement perturbative QCD calculations. Their difference is translated into different assumptions for the form factor  $H(q^2)$ , Kagan and Petrov [5] assume  $H(q^2) \approx \text{const} \approx 1.7 \text{ GeV}^{-1}$ , Ali and Parkhomenko related  $H(q^2)$  to the expansion of the two light-cone distribution amplitudes (LCDA) describing the quark and gluon components of the  $\eta'$  wave function. Fig. 7 shows the measured  $dn/dZ$  distribution, compared with three representative choices for  $H(q^2)$ .  $H(q^2) = H_0 = 1.7 \text{ GeV}^{-1}$ ,  $H_{as}$ , based on the asymptotic form of the  $\eta'$  meson LCDA, and  $H(q^2)$  corresponding to the spectrum with the Gegenbauer coefficients from the best fit range obtained by Ali and Parkhomenko [13], using the previous CLEO II data and the constraints from the  $\eta' - \gamma$  transitions [10]. Note that most of the discrepancy between theory and data occurs in the  $Z = 0.7$  bin. In



fact, the  $\chi^2$  for the fit of the new data with this theoretical parametrization is 27. This may imply that higher order terms in the QCD expansion need to be taken into account, or that the  $\Upsilon(1S) \rightarrow 3g$  is not the dominant source of  $\eta'$ , at least at a scaled energy as high as  $Z = 0.7$ .

In conclusion we have measured the energy spectra of the  $\eta'$  meson in the decay  $\Upsilon(1S) \rightarrow \eta'X$ . Our results are not very well described by existing models based on strong gluonic coupling of the  $\eta'$ . Thus the observed  $B \rightarrow \eta'X$  inclusive branching fraction is unlikely to be explained by an enhanced  $g^*g\eta'$  form factor, and an explanation outside the realm of the Standard Model may be needed to account for this large rate.

#### IV. ACKNOWLEDGEMENTS

We would like to thank A. Kagan and A. Ali for useful discussions and for providing us with their calculations. We gratefully acknowledge the effort of the CESR staff in providing us with excellent luminosity and running conditions. D. Cronin-Hennessy and A. Ryd thank the A.P. Sloan Foundation. This work was supported by the National Science Foundation, the U.S. Department of Energy, and the Natural Sciences and Engineering Research Council of Canada.

- 
- [1] T. E. Browder *et al.* [CLEO Collaboration], Phys. Rev. Lett. **81**, 1786 (1998), [hep-ex/9804018].
  - [2] G. Bonvicini *et al.* [CLEO Collaboration], Phys. Rev. D **68**, 011101 (2003) [hep-ex/0303009].
  - [3] B. Aubert *et al.* [BABAR Collaboration], [hep-ex/0109034]; B. Aubert *et al.* [BABAR Collaboration], Phys. Rev. Lett. **93**, 061801 (2004) [hep-ex/0401006].
  - [4] D. Atwood and A. Soni, Phys. Lett. B **405**, 150 (1997) [hep-ph/9704357].
  - [5] A. L. Kagan (2002), [hep-ph/0201313].
  - [6] A. Ali and A. Y. Parkhomenko, Phys. Rev. D **65**, 074020 (2002) [hep-ph/0012212].
  - [7] W. S. Hou and B. Tseng, Phys. Rev. Lett. **80**, 434 (1998) [hep-ph/9705304].
  - [8] A. Kagan and A. A. Petrov [hep-ph/9707354].
  - [9] T. Muta and M. Z. Yang, [hep-ph/9909484].
  - [10] P. Kroll and K. Passek-Kumericki, Phys. Rev. D **67**, 054017 (2003)[hep-ph/0210045].
  - [11] H. Albrecht *et al.* [ARGUS Collaboration], Z. Phys. C **58**, 199 (1993).
  - [12] M. Artuso *et al.* [CLEO Collaboration], Phys. Rev. D **67**, 052003 (2003).
  - [13] A. Ali and A. Y. Parkhomenko, Eur. Phys. J. C **30**, 183 (2003) [hep-ph/0304278].
  - [14] D. Peterson *et al.*, Nucl. Instrum. Meth. A **478**, 142 (2002).
  - [15] Y. Kubota *et al.*, Nucl. Instrum. Meth. A **320**, 66 (1992).
  - [16] M. Artuso *et al.*, Nucl. Instrum. Meth. A **502**, 91 (2003) [hep-ex/0209009].
  - [17] R. Ammar *et al.* [CLEO Collaboration], Phys. Rev. D **57**, 1350 (1998) [hep-ex/9707018].
  - [18] Particle Data Group, S. Eidelemann *et al.*, Phys. Lett. **B**, 1 (2004) and 2005 partial update for edition 2006 (url; <http://pdg.lbl.gov>).
  - [19] R. Brun *et al.*, computer code GEANT3.21, CERN Program Library Long Write Up W5013 (1992).
  - [20] R. Kleiss and S. van der Marck, Nucl. Phys. B **342**, 61 (1990).

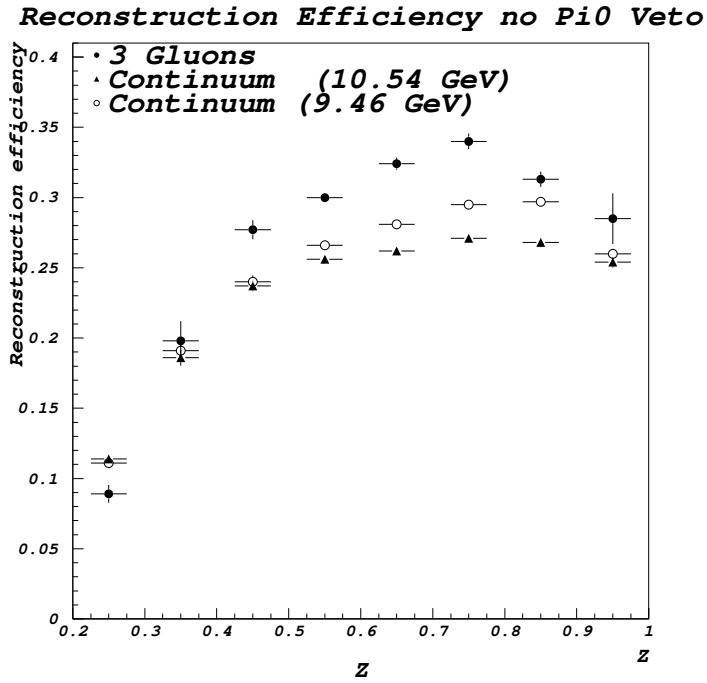


FIG. 4: The  $\eta'$  reconstruction efficiencies as function of  $Z$  for different MC samples with no  $\pi^0$  veto, and with  $\pi^0$  veto in photon selection. The  $\pi^0$  veto was applied in this analysis for  $Z < 0.5$ .

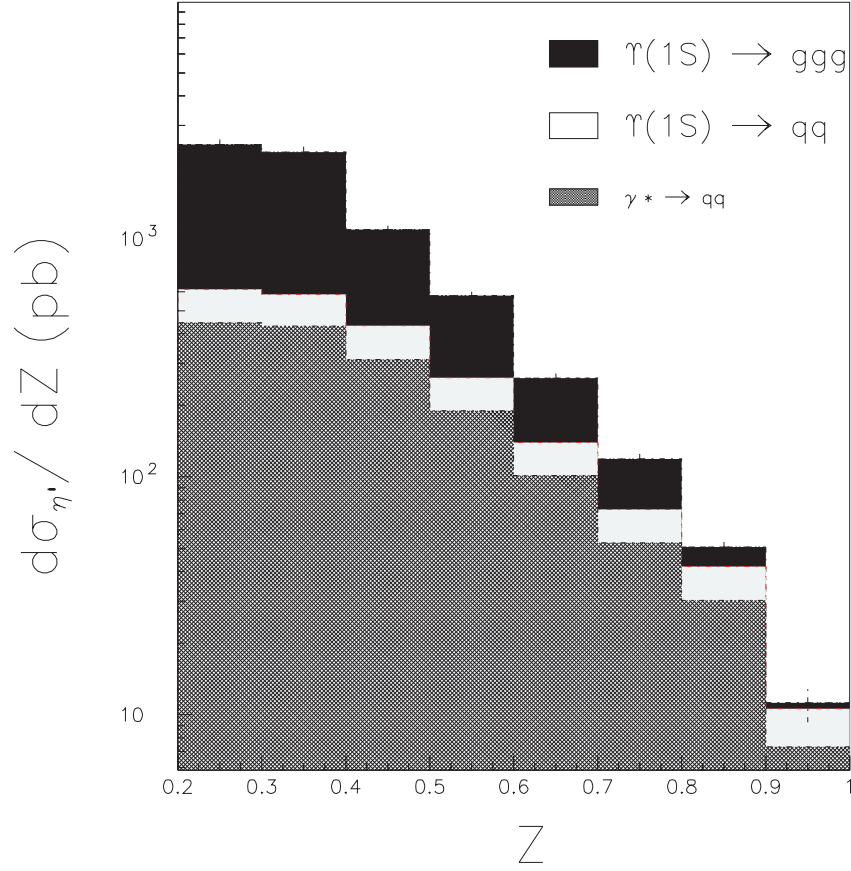


FIG. 5: The differential cross sections  $d\sigma/dZ$  a)  $\gamma^* \rightarrow q\bar{q} \rightarrow \eta'X$  (hatched), b)  $\Upsilon(1S) \rightarrow q\bar{q} \rightarrow \eta'X$  (white) and c)  $\Upsilon(1S) \rightarrow ggg \rightarrow \eta'X$  (black).

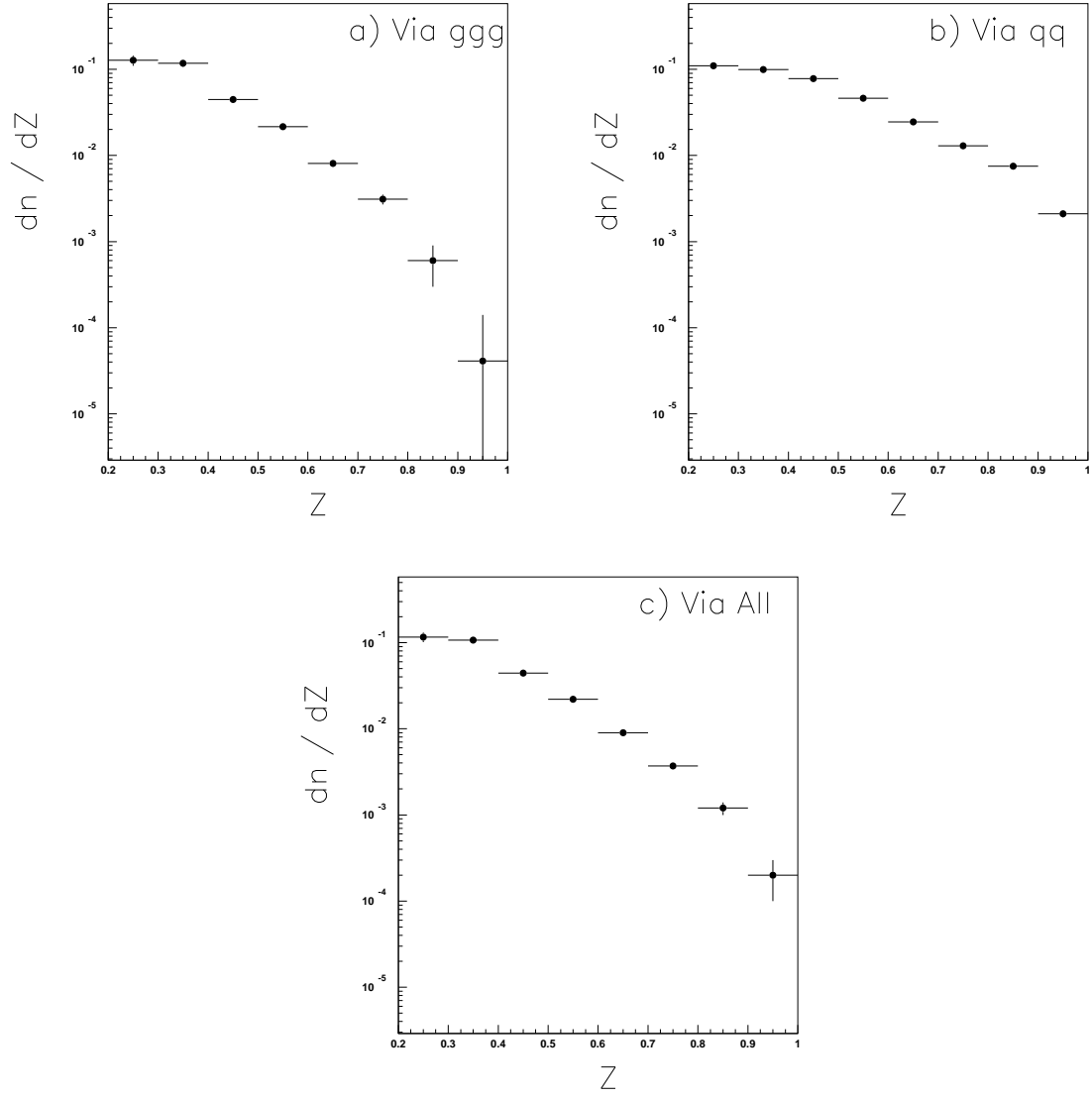


FIG. 6: The energy distribution function  $dn/dZ$  as defined in context for a)  $\Upsilon(1S) \rightarrow ggg \rightarrow \eta' X$ , b)  $\Upsilon(1S) \rightarrow q\bar{q} \rightarrow \eta' X$ , and c)  $\Upsilon(1S) \rightarrow \eta' X$ .

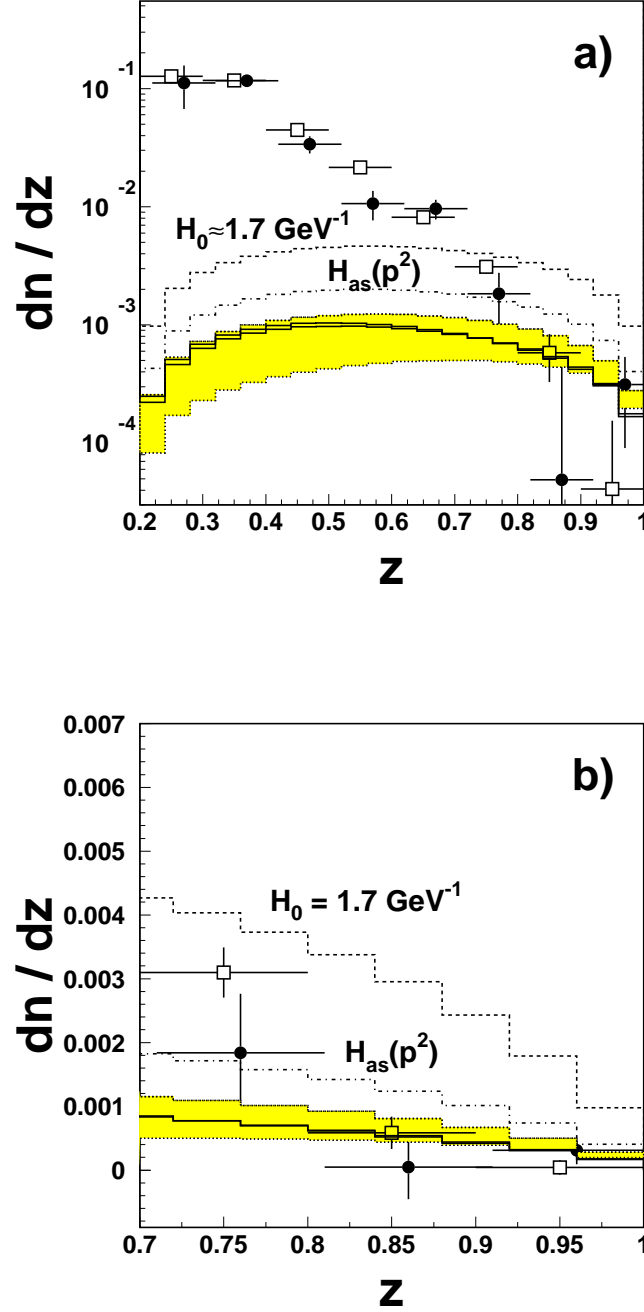


FIG. 7: Energy spectrum of the  $\eta'$ -meson in the decay  $\Upsilon(1S) \rightarrow \eta'X$ : measured spectra: open squares correspond to the data presented in this paper, filled circles are the previously reported CLEO II data [12]:a) measured spectra b)  $Z \geq 0.7$  region zoomed in to show the comparison with the theoretical predictions more clearly. The dashed curve corresponds to a constant value of the function  $H(p^2) = H_0 \simeq 1.7 \text{ GeV}^{-1}$ , and the dash-dotted curve ( $H_{as}(p^2)$ ) corresponds to the asymptotic form of the  $\eta'$ -meson LCDA [12] (i.e.,  $B_2^{(g)} = 0$  and  $B_2^{(g)} = 0$ ). The spectrum with the Gegenbauer coefficients in the combined best-fit range of these parameters is shown in the shaded region. The solid curve corresponds to the best fit values of the Gegenbauer coefficients from the analysis of the  $\Upsilon(1S) \rightarrow \eta'X$  CLEO II data alone. The dotted points represent the CLEO II data [13] and the boxed points represent the CLEO III data.